

Forward $J/\psi + J/\psi$ and $J/\psi + \psi'$ production with High Energy Factorization

S.P. Baranov¹, A.V. Lipatov^{2,3}, M.A. Malyshev^{2,4},
A.A. Prokhorov³, P.M. Zhang⁵

May 29, 2024

¹*P.N. Lebedev Institute of Physics, Moscow 119991, Russia*

²*Skobeltsyn Institute of Nuclear Physics, Lomonosov Moscow State University, Moscow 119991, Russia*

³*Joint Institute for Nuclear Research, Dubna 141980, Moscow region, Russia*

⁴*Moscow Aviation Institute, Moscow 125993, Russia*

⁵*School of Physics and Astronomy, Sun Yat-sen University, Zhuhai 519082, China*

Abstract

We calculate the cross sections of associated $J/\psi + \psi'$ and $J/\psi + J/\psi$ production in pp collisions at $\sqrt{s} = 13$ TeV in the forward kinematic region. The High Energy Factorization (k_T -factorization) framework supplemented with the Catani-Ciafaloni-Fiorani-Marchesini evolution of gluon densities in a proton is applied. We demonstrate that latest data on $J/\psi + J/\psi$ production and first experimental data on $J/\psi + \psi'$ events taken very recently by the LHCb Collaboration can be described well by the color singlet terms and contributions from the double parton scattering (DPS) with the standard choice for σ_{eff} parameter. The relative production rate $\sigma(J/\psi + \psi')/\sigma(J/\psi + J/\psi)$ is found to be sensitive to the DPS terms as well as to feeddown contributions.

Keywords: heavy quarkonia, high-energy factorization, CCFM evolution, TMD gluon densities, double parton scattering

Inclusive and associated production of quarkonium states in hadron-hadron collisions at high energies attracts much attention from both theoretical and experimental sides. It probes Quantum Chromodynamics (QCD) in perturbative and non-perturbative regimes and provides important information about the interaction dynamics. New data, as soon as they appear, trigger theoretical activity aimed at their understanding and description. Our present note is motivated by the first measurement [1] of the associated $J/\psi + \psi'$ production and very recent data [2] on $J/\psi + J/\psi$ production in pp collisions taken by the LHCb Collaboration in the forward kinematic region at $\sqrt{s} = 13$ TeV. These data include contributions from both single and double parton scattering production mechanisms (SPS and DPS, respectively). The data on $J/\psi + \psi'$ events present the differential cross sections as functions of several kinematic variables, namely, the rapidity and azimuthal angle differences between the J/ψ and ψ' mesons $\Delta y(J/\psi, \psi')$ and $\Delta\phi(J/\psi, \psi')$, the transverse momentum $p_T(J/\psi, \psi')$, rapidity $y(J/\psi, \psi')$ and invariant mass $M(J/\psi, \psi')$ of the $J/\psi + \psi'$ system. Similar observables as well as transverse momentum, rapidity of either J/ψ meson and transverse momentum asymmetry \mathcal{A}_T of the two J/ψ mesons have been investigated in the latest $J/\psi + J/\psi$ analysis [2]. Moreover, the relative production rate $\sigma(J/\psi + \psi')/\sigma(J/\psi + J/\psi)$ has been reported [1] for the first time.

A commonly accepted framework for the description of heavy quarkonia production and decays is provided by non-relativistic QCD (NRQCD) approximation [3, 4]. Explicit calculations [5] show that the main role in the production of quarkonium pairs at forward rapidities is played by the color singlet (CS) mechanism, whereas the color octet (CO) contributions are much smaller. The tree-level next-to-leading order (NLO*) CS calculations for SPS mechanism performed with the HELAC-ONIA tool [6, 7] tend to overestimate the LHCb data [1], especially at low $\Delta y(J/\psi, \psi')$, low $M(J/\psi, \psi')$ and moderate $p_T(J/\psi, \psi')$, though still remain consistent with them within the large theoretical uncertainties. The latest data [2] on forward $J/\psi + J/\psi$ events can also be described by the NLO* CS calculations within the large uncertainties, although the DPS contributions were not subtracted from the measurements¹.

In the present note we analyse the LHCb data [1, 2] on double charmonia production in the framework of the k_T -factorization [10] or, equivalently, the High Energy Factorization [11] formalism. This formalism has certain technical advantages in the ease of including higher-order radiative corrections that can be taken into account in the form of transverse momentum dependent (TMD) gluon distributions in a proton². Recently, it has been successfully applied to the double J/ψ production at the LHC [13–15]. In particular, it was demonstrated [14, 15] that the early data on $J/\psi + J/\psi$ events collected at $\sqrt{s} = 7$ and 13 TeV at forward rapidities can be described well by the sum of color-singlet SPS and DPS mechanisms. It was also confirmed that the CO contributions at the LHC conditions can be safely omitted in the region of small invariant masses $M(J/\psi, J/\psi)$ in the forward rapidity region. Now, in addition to J/ψ pairs, we consider $J/\psi + \psi'$ production. Our study is even more stimulated by the fact that previous theoretical attempts [6, 7, 9, 16] were not fairly successful.

We preserve full consistency with our previous investigations [13–15] and employ the k_T -factorization QCD approach [10, 11], as it was mentioned above. This approach is based on the Balitsky-Fadin-Kuraev-Lipatov (BFKL) [17] or Catani-Ciafaloni-Fiorani-Marchesini (CCFM) [18] gluon evolution equations and can be used as a convenient alternative to explicit higher-order pQCD calculations.

¹The leading-order (LO) NRQCD predictions $J/\psi + J/\psi$ production are known [8] and the NLO* contributions to the CS and CO mechanisms have been calculated [9].

²See, for example, review [12] for more information.

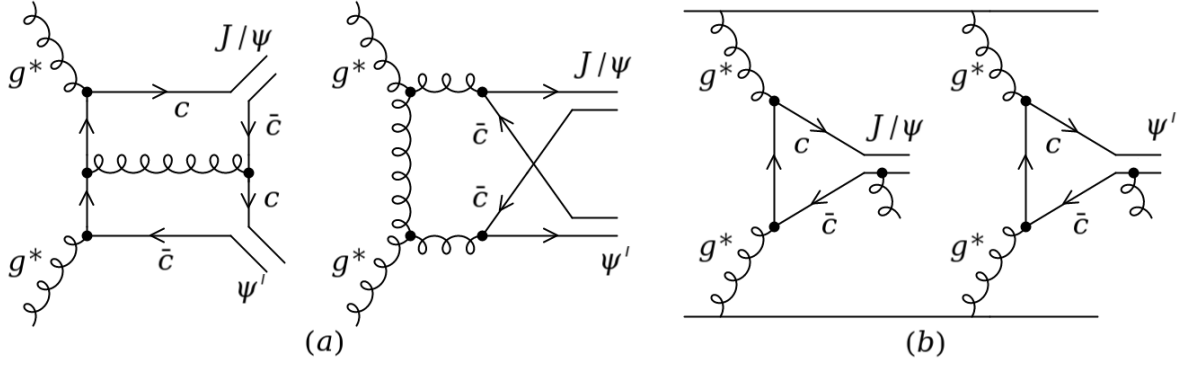


Figure 1: Examples of Feynman diagrams, contributing to the CS production of charmonium pairs.

In the NRQCD framework, the colliding gluons produce heavy quark-antiquark pairs which further evolve into real mesons. At forward rapidities, the leading CS contribution to associated $J/\psi + J/\psi$ or $J/\psi + \psi'$ production is represented by an $\mathcal{O}(\alpha_s^4)$ partonic subprocess

$$g^*(k_1) + g^*(k_2) \rightarrow c\bar{c} \left[{}^3S_1^{(1)} \right] (p_1) + c\bar{c} \left[{}^3S_1^{(1)} \right] (p_2), \quad (1)$$

where the four-momenta of all particles are indicated in the parentheses. This subprocess includes also feeddown contributions (namely, $J/\psi + \psi'$ and/or $\psi' + \psi'$ production), where excited charmonium state ψ' decays into J/ψ meson. Other subleading subprocesses which involve the production of intermediate P -wave states and/or additional gluons (see [15] for more details) were found to be small and not taken into account here. In accordance with the k_T -factorization, the initial gluons have nonzero transverse momenta $k_1^2 \equiv -\mathbf{k}_{1T}^2 \neq 0$, $k_2^2 \equiv -\mathbf{k}_{2T}^2 \neq 0$ and are off-shell. Some examples of the relevant Feynman diagrams are shown in Fig. 1.

The gauge invariant expression for off-shell (depending on the virtualities of incoming gluons) production amplitude (1) has been calculated earlier [13]. It contains spin and color projection operators [19–23] which guarantee the proper quantum numbers of the final state charmonia. In the NRQCD approximation which we are using the meson mass must be strictly equal to the sum of the constituent quark masses. However, this cannot be fulfilled simultaneously for both J/ψ and ψ' . So that, for the associated $J/\psi + \psi'$ production we used a compromise value $m_c = (m_{J/\psi} + m_{\psi'})/4$ (see discussion below). In all other respects our present theoretical scheme is identical to that used in previous studies [13–15]. We only note that the initial gluon spin density matrix is taken in the form of so called "non-sense gauge", namely, $\sum \epsilon^\mu \epsilon^{*\nu} = \mathbf{k}_T^\mu \mathbf{k}_T^\nu / \mathbf{k}_T^2$. This expression converges to the ordinary $-g^{\mu\nu}/2$ in the collinear limit $\mathbf{k}_T \rightarrow 0$ after averaging over the azimuthal angle.

According to the k_T -factorization prescription [10, 11], the contribution from CS production mechanism (1) to $J/\psi + \psi'$ cross section is calculated as a convolution of the corresponding off-mass shell production amplitudes and TMD gluon densities in a proton:

$$\begin{aligned} \sigma(pp \rightarrow J/\psi + \psi' + X) &= \int \frac{1}{16\pi(x_1 x_2 s)^2} |\bar{\mathcal{A}}(g^* + g^* \rightarrow J/\psi + \psi')|^2 \times \\ &\times f_g(x_1, \mathbf{k}_{1T}^2, \mu^2) f_g(x_2, \mathbf{k}_{2T}^2, \mu^2) d\mathbf{k}_{1T}^2 d\mathbf{k}_{2T}^2 d\mathbf{p}_{1T}^2 dy_1 dy_2 \frac{d\phi_1}{2\pi} \frac{d\phi_2}{2\pi} \frac{d\psi_1}{2\pi}, \end{aligned} \quad (2)$$

where ψ_1 is the azimuthal angle of the outgoing J/ψ meson, ϕ_1 and ϕ_2 are the azimuthal angles of the initial off-shell gluons having the longitudinal momentum fractions x_1 and x_2 , y_1 and y_2 are the center of mass rapidities of the produced particles. Note that the cross section of associated $J/\psi + J/\psi$ production can be calculated in a similar way. Here $f_g(x, \mathbf{k}_T^2, \mu^2)$ is the TMD gluon density in a proton taken at the scale μ^2 . For the latter, we have tried two recent sets, referred to as JH'2013 set 2 [24] and LLM'2022 [25]. These gluon densities have been obtained from a numerical solution of the CCFM equation and are now widely used in phenomenological applications (see, for example, [26–30] and references therein). The parameters of (rather empirical) input distributions employed in the JH'2013 gluon were derived from a fit to the HERA data on the proton structure functions $F_2(x, Q^2)$ and $F_2^c(x, Q^2)$ at small x . An analytical expression for the input gluon density in the very recent LLM'2022 set was suited to the best description of the LHC data on the charged hadron production at low transverse momenta in the framework of modified soft quark-gluon string model [31, 32] with taking into account the gluon saturation effects important at low scales. The necessary phenomenological parameters were deduced from the LHC and HERA data on several hard QCD processes (see [25] for more information). Both the JH'2013 set 2 and LLM'2022 gluon distributions are available from the popular TMDLIB package [33] and Monte-Carlo generator PEGASUS [34].

In addition to the above, we also take into account the contributions from DPS mechanism, which is now widely discussed in the literature. In contrast with SPS subprocess (1), where every quarkonium pair is produced in a single gluon-gluon collision, the DPS events originate from two independent parton interactions and are expected to be important at forward rapidities (see, for example, [35–37]). We apply a commonly used factorization formula:

$$\sigma_{\text{DPS}}(pp \rightarrow \mathcal{Q}_1 + \mathcal{Q}_2 + X) = \frac{m}{2} \frac{\sigma(pp \rightarrow \mathcal{Q}_1 + X)\sigma(pp \rightarrow \mathcal{Q}_2 + X)}{\sigma_{\text{eff}}}, \quad (3)$$

where $\mathcal{Q}_i = J/\psi, \psi'$ or χ_{cJ} and σ_{eff} is the effective cross section which represents the degree of overlap in the transverse space between two partonic interactions that constitute the DPS process. Note that $m = 1$ if $\mathcal{Q}_1 = \mathcal{Q}_2$ and $m = 2$ if \mathcal{Q}_1 and \mathcal{Q}_2 are different, thus preventing double counting for identical particles. The effective DPS cross section can be considered as a normalization constant which incorporates all "DPS unknowns" into a single phenomenological parameter. The derivation of formula (3) relies on two approximations: first, the double parton distribution function can be decomposed into longitudinal and transverse components and, second, the longitudinal component reduces to the diagonal product of two independent single parton densities. The latter is generally acceptable for the conditions of LHCb experiment. The inclusive cross sections $\sigma(pp \rightarrow J/\psi + X)$ and/or $\sigma(pp \rightarrow \psi' + X)$ involved in (3) are calculated within the NRQCD framework supplemented with k_T -factorization (see, for example, [38] and references therein). The effective cross section is chosen as $\sigma_{\text{eff}} = 15$ mb, which is a commonly accepted value³. Our calculation incorporates all possible feeddown contributions to the DPS cross section except the χ_{c0} production due to its low branching fraction to the J/ψ .

The meson masses were taken in our calculations as $m(J/\psi) = 3.096$ GeV, $m(\chi_{c1}) = 3.511$ GeV, $m(\chi_{c2}) = 3.556$ GeV and $m(\psi') = 3.686$ GeV (see [43]). A complete list of used CS and CO LDMEs can be found [15]. The branching fractions are $Br(\chi_{c1} \rightarrow J/\psi + \gamma) = 0.339$, $Br(\chi_{c2} \rightarrow J/\psi + \gamma) = 0.192$ and $Br(\psi' \rightarrow J/\psi + X) = 0.529$. The renormalization

³A very close value $\sigma_{\text{eff}} = 13.8$ mb has been extracted [14] from a fit to the LHCb data on the double J/ψ production. However, some other works on the double quarkonia production may seem to favor much smaller values: $\sigma_{\text{eff}} \sim 5$ mb [39–42]. We argue that this could be due to an incomplete treatment of the SPS contributions, see [14] for more details.

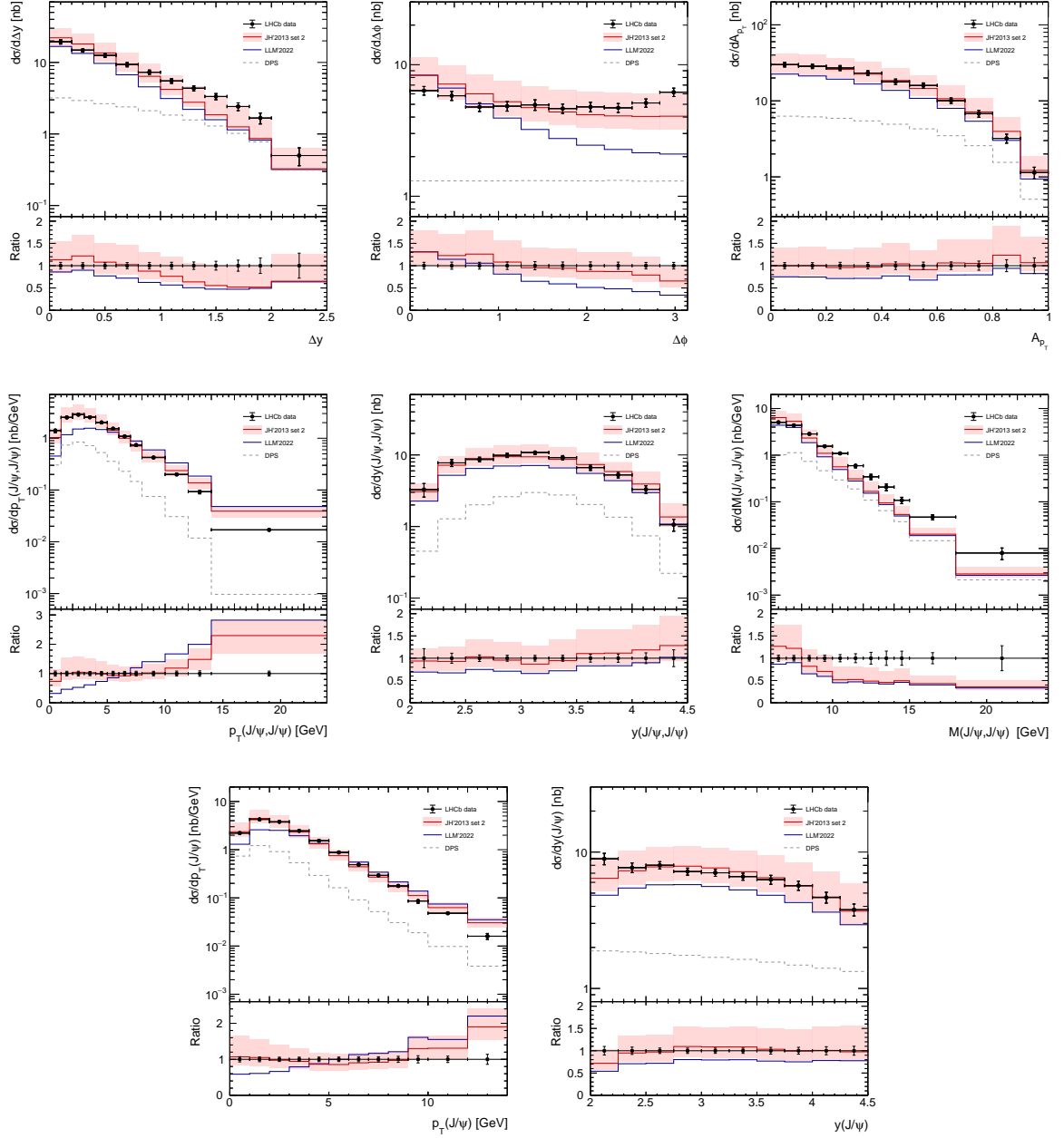


Figure 2: Differential cross sections of forward $J/\psi + J/\psi$ production at $\sqrt{s} = 13$ TeV as functions of their rapidity difference $\Delta y(J/\psi, J/\psi)$, azimuthal angle difference $\Delta\phi(J/\psi, J/\psi)$, transverse momentum asymmetry \mathcal{A}_T , transverse momentum $p_T(J/\psi, J/\psi)$, rapidity $y(J/\psi, J/\psi)$, invariant mass $M(J/\psi, J/\psi)$ and transverse momentum $p_T(J/\psi)$ and rapidity $y(J/\psi)$ of either of J/ψ meson. Separately shown contributions from the DPS production mechanism. The data are of LHCb [2].

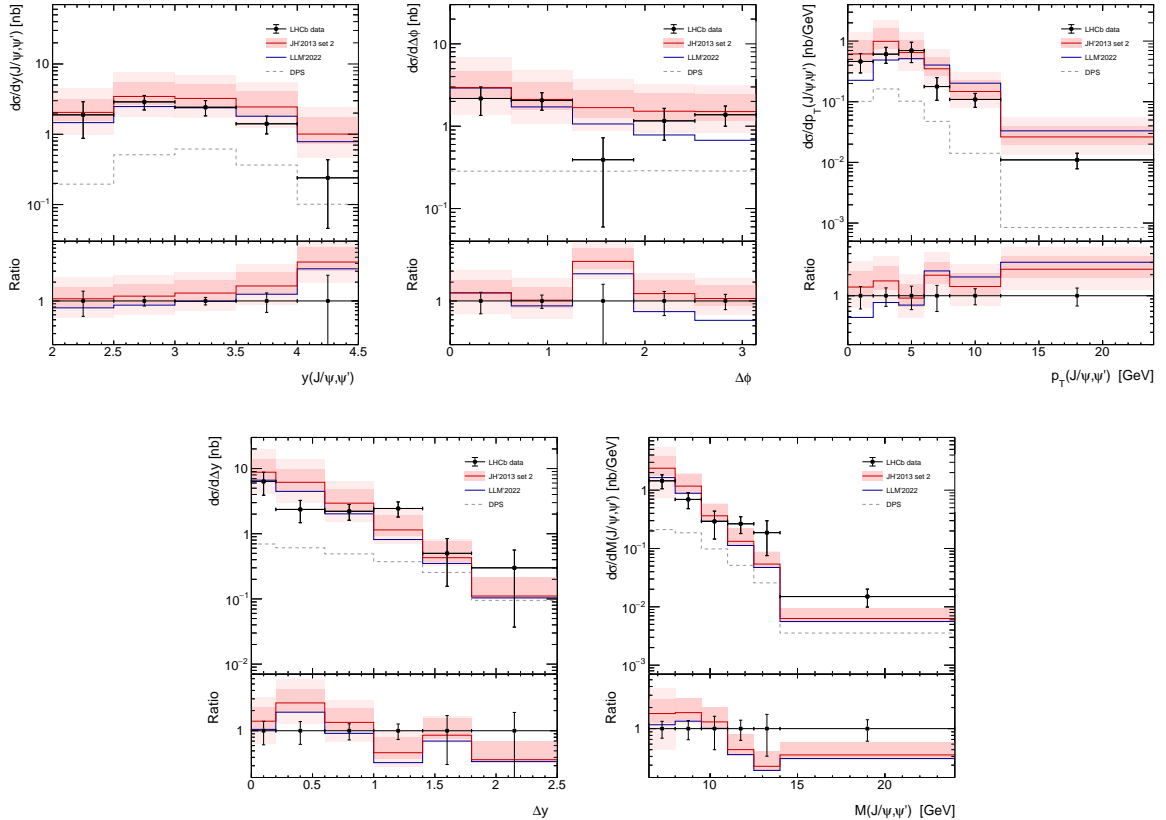


Figure 3: Differential cross sections of associated J/ψ and ψ' production as functions of their rapidity difference $\Delta y(J/\psi, \psi')$, azimuthal angle difference $\Delta\phi(J/\psi, \psi')$, transverse momentum $p_T(J/\psi, \psi')$, rapidity $y(J/\psi, \psi')$ and invariant mass $M(J/\psi, \psi')$. Separately shown are the contributions from DPS production mechanism. The data are of LHCb [1].

and factorization scales were calculated as $\mu_R^2 = \mu_F^2 = \xi^2(\hat{s} + \mathbf{Q}_T^2)$, where \mathbf{Q}_T is the total transverse momentum of the initial off-shell gluon pair. This choice observes full consistency with our previous work [14] and is dictated by the CCFM evolution. It comes from the kinematics of gluon radiation, namely from the gluon angular ordering condition. The quantity $\hat{s} + \mathbf{Q}_T^2$ describes the phase space available for the (angular ordered) gluon radiation and sets the upper bound both for the emitted and exchanged transverse momentum (see [18] for more information). We use a two-loop formula for QCD strong coupling with $N_f = 4$ active quark flavours and $\Lambda_{\text{QCD}} = 200$ MeV. To estimate the theoretical uncertainties of our calculations, we varied the parameter ξ between 1/2 and 2.

Our simulations closely follow the experimental setup [1, 2]. In particular, the produced J/ψ and ψ' mesons are required to be in the region of $2 < y < 4.5$ and $p_T < 14$ GeV, where y is the rapidity of a final state particle. All these conditions have been implemented in our numerical program.

The results of our calculations of the differential cross sections for forward $J/\psi + J/\psi$ and $J/\psi + \psi'$ production are shown in Figs. 2 and 3, respectively. The theoretical uncertainty bands (represented by the shaded regions) are shown for JH'2013 set 2 gluon density and related with scale uncertainties, which have been estimated in a usual way, by varying the ξ parameter around its default value $\xi = 1$ by a factor of 2. This was accompanied with using the JH'2013 set 2+ and JH'2013 set 2- gluon densities in place of default distribution, in accordance with [24]. We also include the mass uncertainties for

CS $J/\psi + \psi'$ subprocess by varying the c-quark mass between $m(J/\psi)/2 < m_c < m(\psi')/2$. These effects are added in quadratures with scale uncertainties and represented by the light shaded bands in Fig. 3. To highlight the role of DPS mechanism, we separately show the corresponding contributions. One can see that our predictions agree well with the latest LHCb data. The only exception is seen at larger invariant masses $M(J/\psi, J/\psi)$ and $M(J/\psi, \psi')$, where the calculated cross sections systematically underestimate the experimental results. Note that still additional contributions related to multiple gluon radiation in the initial gluon evolution cascade⁴ could play a role at large $M(J/\psi, J/\psi)$ and $M(J/\psi, \psi')$. However, an accurate account of all these terms needs rather lengthy numerical calculations and is therefore left out of our present scope.

We find special interest in the correlation observables $\Delta\phi(J/\psi, \psi')$, $\Delta\phi(J/\psi, J/\psi)$ and in the p_T balance observables $p_T(J/\psi, J/\psi)$ and $p_T(J/\psi, \psi')$ as they are known to be particularly sensitive to the non-collinear gluon evolution dynamics in a proton (see, for example, [44] and references therein). We point out a good description (within the uncertainties) of all these distributions with the JH'2013 set 2 gluon density. The LLM-based predictions, in general, tend to slightly underestimate the LHCb data [1, 2] and JH'2013 set 2 predictions. In fact, the measured fiducial cross sections of forward $J/\psi + J/\psi$ and $J/\psi + \psi'$ production are $\sigma(J/\psi + J/\psi) = 16.36 \pm 0.92$ nb and $\sigma(J/\psi + \psi') = 4.5 \pm 0.8$ nb. They can be compared with the JH'2013 set 2 and LLM'2022 results, which are $\sigma^{\text{JH}}(J/\psi + J/\psi) = 16.2^{+7.2}_{-3.5}$ (scale unc.) nb, $\sigma^{\text{JH}}(J/\psi + \psi') = 6.1^{+3.7}_{-1.5}$ (scale unc.) $^{+6.2}_{-2.6}$ (mass unc.) nb and $\sigma^{\text{LLM}}(J/\psi + J/\psi) = 12.1^{+4.9}_{-2.3}$ (scale unc.) nb, $\sigma^{\text{LLM}}(J/\psi + \psi') = 4.5^{+2.5}_{-0.9}$ (scale unc.) $^{+4.3}_{-1.8}$ (mass unc.) nb, respectively. Moreover, one can see a clear difference between the JH'2013 set 2 and LLM'2022 predictions in the shape of azimuthal angle correlations and transverse momenta correlations of the produced mesons. It demonstrates again that such observables could be useful to discriminate the different TMD evolution scenarios.

The estimated contributions from the DPS production mechanism are typically small and only become important in some specific regions like low $p_T(J/\psi, J/\psi)$, $p_T(J/\psi, \psi')$ and large $M(J/\psi, J/\psi) \geq 15$ GeV, $M(J/\psi, \psi') \geq 15$ GeV, $|\Delta y(J/\psi, J/\psi)| \geq 1.5$, $|\Delta y(J/\psi, \psi')| \geq 1.5$. Our calculations clearly show that taking these terms into account improves the quality of the data description and becomes necessary in the forward kinematic region. The role of DPS and feeddown contributions is exhibited in Fig. 4, where the ratio $\sigma(J/\psi + \psi')/\sigma(J/\psi + J/\psi)$ is shown as a function of the different kinematic variables. We find that the relative production rate is very sensitive to the DPS and feeddown yields⁵. Finally, we can conclude that the first LHCb measurement [1] of the associated $J/\psi + \psi'$ production and the very recent experimental data [2] on $J/\psi + J/\psi$ production at $\sqrt{s} = 13$ TeV can be well described by the color singlet SPS mechanism and DPS contributions calculated with the standard choice of σ_{eff} parameter.

Acknowledgements. A.V.L. and M.A.M. would like to thank School of Physics and Astronomy, Sun Yat-sen University (Zhuhai, China) for warm hospitality. P.M.Z. was partially supported by the National Natural Science Foundation of China (Grant No. 12375084).

References

- [1] LHCb Collaboration, arXiv:2311.15921 [hep-ex].

⁴Such terms are extremely important at central rapidities [14, 15].

⁵Note that only the SPS terms are affected by the choice of TMD gluon density in a proton. The DPS predictions are stable, because when we switch to a different set of TMD gluons we have to accordingly change the LDME values, thus making the net result the same.

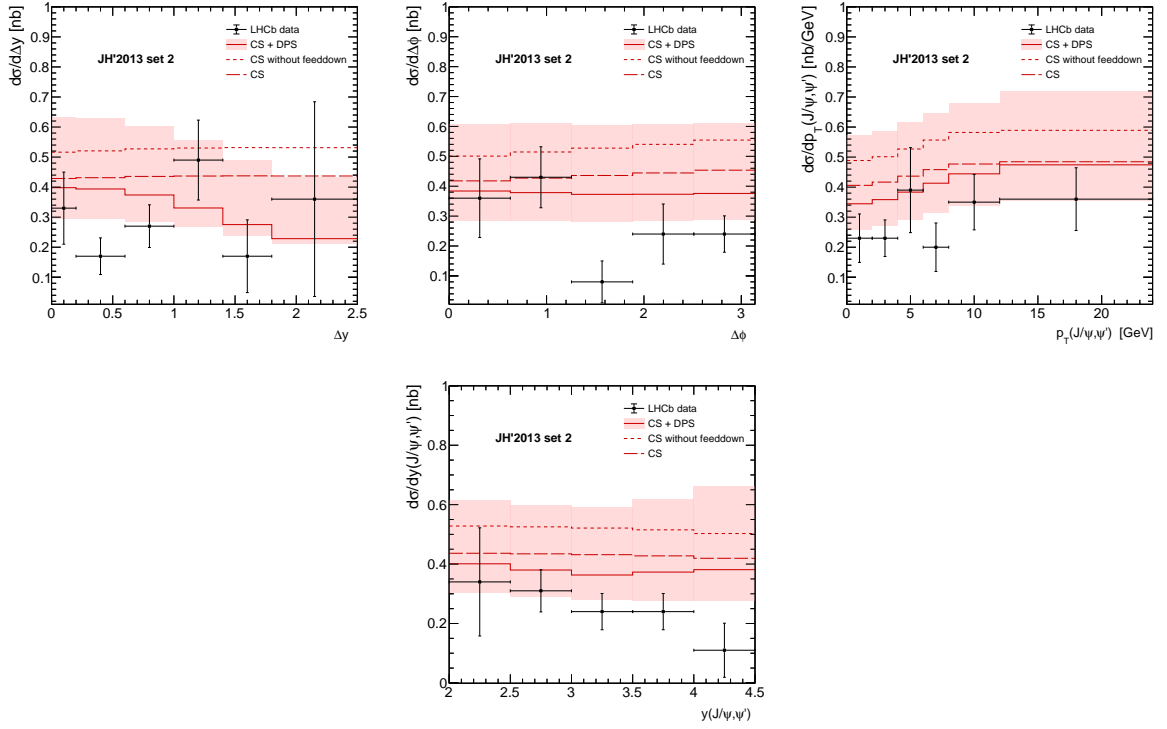


Figure 4: Relative production rate $\sigma(J/\psi + \psi')/\sigma(J/\psi + J/\psi)$ calculated at $\sqrt{s} = 13$ TeV as a function of several kinematic variables. The data are of LHCb [1].

- [2] LHCb Collaboration, JHEP **03**, 088 (2024).
- [3] G. Bodwin, E. Braaten, G. Lepage, Phys. Rev. D **51**, 1125 (1995).
- [4] P. Cho, A.K. Leibovich, Phys. Rev. D **53**, 150 (1996);
P. Cho, A.K. Leibovich, Phys. Rev. D **53**, 6203 (1996).
- [5] J.-P. Lansberg, H.-S. Shao, N. Yamanaka, Y.-J. Zhang, Eur. Phys. J. C **79**, 1006 (2019).
- [6] H.-S. Shao, Comput. Phys. Commun. **184**, 2562 (2013).
- [7] H.-S. Shao, Comput. Phys. Commun. **198**, 238 (2016).
- [8] Z.-G. He, B.A. Kniehl, Phys. Rev. Lett. **115**, 022002 (2015).
- [9] J.-P. Lansberg, H.-S. Shao, Phys. Rev. Lett. **111**, 122001 (2013).
- [10] L.V. Gribov, E.M. Levin, M.G. Ryskin, Phys. Rep. **100**, 1 (1983);
E.M. Levin, M.G. Ryskin, Yu.M. Shabelsky, A.G. Shuvaev, Sov. J. Nucl. Phys. **53**, 657 (1991).
- [11] S. Catani, M. Ciafaloni, F. Hautmann, Nucl. Phys. B **242**, 97 (1990);
S. Catani, M. Ciafaloni, F. Hautmann, Nucl. Phys. B **366**, 135 (1991);
J.C. Collins, R.K. Ellis, Nucl. Phys. B **360**, 3 (1991).
- [12] R. Angeles-Martinez, A. Bacchetta, I.I. Balitsky, D. Boer, M. Boglione, R. Boussarie, F.A. Ceccopieri, I.O. Cherednikov, P. Connor, M.G. Echevarria, G. Ferrera, J. Grados Luyando, F. Hautmann, H. Jung, T. Kasemets, K. Kutak, J.P. Lansberg, A. Lelek,

- G.I. Lykasov, J.D. Madrigal Martinez, P.J. Mulders, E.R. Nocera, E. Petreska, C. Pisano, R. Placakyte, V. Radescu, M. Radici, G. Schnell, I. Scimemi, A. Signori, L. Szymanowski, S. Taheri Monfared, F.F. Van der Veken, H.J. van Haevermaet, P. Van Mechelen, A.A. Vladimirov, S. Wallon, *Acta Phys. Polon. B* **46**, 2501 (2015).
- [13] S.P. Baranov, *Phys. Rev. D* **84**, 054012 (2011).
- [14] A.A. Prokhorov, A.V. Lipatov, M.A. Malyshev, S.P. Baranov, *Eur. Phys. J. C* **80**, 1046 (2020).
- [15] S.P. Baranov, A.V. Lipatov, A.A. Prokhorov, *Phys. Rev. D* **106**, 034020 (2022).
- [16] Z.-G. He, B.A. Kniehl, M.A. Nefedov, V.A. Saleev, *Phys. Rev. Lett.* **123**, 162002 (2019).
- [17] E.A. Kuraev, L.N. Lipatov, V.S. Fadin, *Sov. Phys. JETP* **44**, 443 (1976);
E.A. Kuraev, L.N. Lipatov, V.S. Fadin, *Sov. Phys. JETP* **45**, 199 (1977);
I.I. Balitsky, L.N. Lipatov, *Sov. J. Nucl. Phys.* **28**, 822 (1978).
- [18] M. Ciafaloni, *Nucl. Phys. B* **296**, 49 (1988);
S. Catani, F. Fiorani, G. Marchesini, *Phys. Lett. B* **234**, 339 (1990);
S. Catani, F. Fiorani, G. Marchesini, *Nucl. Phys. B* **336**, 18 (1990);
G. Marchesini, *Nucl. Phys. B* **445**, 49 (1995).
- [19] C.-H. Chang, *Nucl. Phys. B* **172**, 425 (1980).
- [20] E.L. Berger, D. Jones, *Phys. Rev. D* **23**, 1521 (1981).
- [21] R. Baier, R. Rückl, *Phys. Lett. B* **102**, 364 (1981).
- [22] H. Krasemann, *Z. Phys. C* **1**, 189 (1979).
- [23] G. Guberina, J. Kühn, R. Peccei, R. Rückl, *Nucl. Phys. B* **174**, 317 (1980).
- [24] F. Hautmann, H. Jung, *Nucl. Phys. B* **883**, 1 (2014).
- [25] A.V. Lipatov, G.I. Lykasov, M.A. Malyshev, *Phys. Rev. D* **107**, 014022 (2023).
- [26] K. Golec-Biernat, L. Motyka, T. Stebel, *Phys. Rev. D* **103**, 034013 (2021).
- [27] A.V. Lipatov, M.A. Malyshev, H. Jung, *Phys. Rev. D* **100**, 034028 (2019).
- [28] A.V. Lipatov, M.A. Malyshev, *Phys. Rev. D* **103**, 094021 (2020).
- [29] A.V. Lipatov, G.I. Lykasov, M.A. Malyshev, *Phys. Lett. B* **839**, 137780 (2023).
- [30] A.V. Lipatov, M.A. Malyshev, *Phys. Rev. D* **108**, 014022 (2023).
- [31] V.A. Bednyakov, G.I. Lykasov, V.V. Lyubushkin, *Europhys. Lett.* **92**, 31001 (2010).
- [32] V.A. Bednyakov, A.A. Grinyuk, G.I. Lykasov, M. Poghosyan, *Int. J. Mod. Phys. A* **27**, 1250042 (2012).

- [33] N.A. Abdulov, A. Bacchetta, S.P. Baranov, A. Bermudez Martinez, V. Bertone, C. Bissolotti, V. Candelise, L.I. Estevez Banos, M. Bury, P.L.S. Connor, L. Favart, F. Guzman, F. Hautmann, M. Hentschinski, H. Jung, L. Keersmaekers, A.V. Kotikov, A. Kusina, K. Kutak, A. Lelek, J. Lidrych, A.V. Lipatov, G.I. Lykasov, M.A. Malyshev, M. Mendizabal, S. Prestel, S. Sadeghi Barzani, S. Sapeta, M. Schmitz, A. Signori, G. Sorrentino, S. Taheri Monfared, A. van Hameren, A.M. van Kampen, M. Vanden Bemden, A. Vladimirov, Q. Wang, H. Yang, *Eur. Phys. J. C* **81**, 752 (2021).
- [34] A.V. Lipatov, M.A. Malyshev, S.P. Baranov, *Eur. Phys. J. C* **80**, 330 (2020).
- [35] S.P. Baranov, A.M. Snigirev, N.P. Zotov, *Phys. Lett. B* **705**, 116 (2011).
- [36] C.H. Kom, A. Kulesza, W.J. Stirling, *Phys. Rev. Lett. B* **107**, 082002 (2011).
- [37] S.P. Baranov, A.M. Snigirev, N.P. Zotov, A. Szczurek, W. Schäfer, *Phys. Rev. D* **87**, 034035 (2013).
- [38] S.P. Baranov, A.V. Lipatov, *Phys. Rev. D* **100**, 114021 (2019).
- [39] D0 Collaboration, *Phys. Rev. D* **90**, 111101(R) (2014).
- [40] D0 Collaboration, *Phys. Rev. Lett* **116**, 082002 (2016).
- [41] ATLAS Collaboration, *Eur. Phys. J. C* **77**, 76 (2017).
- [42] CMS Collaboration, *JHEP* **1705**, 013 (2017).
- [43] PDG Collaboration, *Prog. Theor. Exp. Phys.* 2022, 083C01 (2022).
- [44] S.P. Baranov, A.V. Lipatov, M.A. Malyshev, *Eur. Phys. J. C* **78**, 820 (2018).